A Planar NF–FF Transformation for Quasi-Spherical Antennas using the Innovative Spiral Scanning

F. D'Agostino, F. Ferrara, C. Gennarelli, R. Guerriero, and M. Migliozzi

Dipartimento di Ingegneria Industriale
University of Salerno, via Giovanni Paolo II, 132 - 84084 Fisciano, Italy
fdagostino@unisa.it, flferrara@unisa.it, cgennarelli@unisa.it, rguerriero@unisa.it, mmigliozzi@unisa.it

Abstract ─ An effective probe compensated near-field–far-field (NF–FF) transformation with planar spiral scanning, using a minimum number of NF data, has been experimentally validated. It allows a remarkable measurement time saving, due to the continuous movements of the positioning systems and to the reduced number of needed NF data. Such a technique is based on a nonredundant sampling representation of the voltage acquired by the probe, obtained by using the theoretical foundations of the NF–FF transformations with spiral scans for quasi-spherical antennas. Then, the NF data needed by the plane-rectangular NF–FF transformation are efficiently recovered from those acquired along the spiral, via an optimal sampling interpolation formula.

Index Terms ─ Antenna measurements, near-field – far-field transformation techniques, nonredundant sampling representations, planar spiral scanning.

I. INTRODUCTION

As well-known, near-field–far-field (NF–FF) transformation techniques [1] are widely used to accurately reconstruct the far field radiated by electrically large antennas from NF measurements carried out in an anechoic chamber. Among these techniques, those adopting the planar scannings [2-6] are particularly suitable for high gain antennas radiating pencil beam patterns. Nowadays, one of the hottest topics concerning the NF–FF transformations is the reduction of the measurement time, that is currently very much greater than the computational one. To this end, the nonredundant sampling representations of electromagnetic (EM) fields [7, 8] have been properly used in [3, 4] and [6] to remarkably reduce the number of NF measurements in the plane-rectangular [2] and plane-polar scanning [5], respectively. Another convenient way to reduce the measurement time is, as suggested in [9], the use of NF–FF transformations employing the planar spiral scanning [9-14], which makes faster the NF data acquisition, since it is executed on fly through a continuous linear movement of the probe and a synchronized rotational one of the antenna under test (AUT). Among them, those [11-14] relying on the nonredundant sampling representations of EM fields are even more effective from the measurement time reduction point of view, due to the lower number of NF data and spiral turns. In particular, the two-dimensional nonredundant representation for the voltage measured by the probe on the plane has been obtained by assuming the AUT as enclosed in the smallest sphere and oblate ellipsoid containing it in [11, 12] and [13, 14], respectively. In both the cases, optimal sampling interpolation (OSI) expansions are used to efficiently recover the data needed by the classical plane-rectangular NF–FF transformation [2] from the nonredundant ones collected along the spiral. Recently, NF–FF transformation techniques with helicoidal and spherical spiral scannings have been also proposed. The interested reader can refer to [15] for a complete bibliography.

The aim of this paper is to provide the experimental assessment of the NF–FF transformation with planar spiral scanning [11] using a ball for modelling volumetric (i.e., quasi-spherical) antennas.

II. NONREDUNDANT PROBE VOLTAGE REPRESENTATION ON A PLANE

Let us consider a quasi-spherical AUT, enclosed in the smallest sphere of radius a able to contain it, and a nondirective probe scanning a spiral lying on a plane at a distance d from the AUT centre. Moreover, let us adopt the spherical coordinate system (r, ϑ, φ) to denote an observation point P (Fig. 1). The voltage measured by such a probe has the same effective spatial bandwidth of the AUT field and, hence, the nonredundant sampling representations of EM fields [7] can be applied to it. Accordingly, to get an effective voltage representation along a curve C lying on the plane, it is convenient to adopt a proper parameter η for describing C and to introduce the "reduced voltage" $\tilde{V}(\eta) = V(\eta)\, e^{j\psi(\eta)}$, where $\psi(\eta)$ is a proper phase function and $V(\eta)$ is the voltage V_φ or V_ρ measured by the probe or by the rotated probe, (ρ, φ) being the polar coordinates on the

Submitted On: July 20, 2015
Accepted On: December 13, 2015

plane. The bandlimitation error, occurring when $\tilde{V}(\eta)$ is approximated by a bandlimited function, is negligible as the bandwidth exceeds a critical value W_η [7] and, thus, it can be controlled by choosing the bandwidth equal to $\chi' W_\eta$, $\chi' > 1$ being the enlargement bandwidth factor.

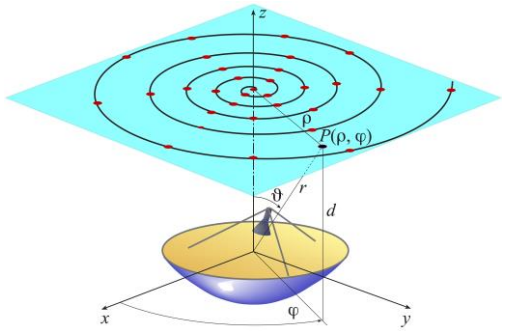

Fig. 1. Planar spiral scanning.

According to the theoretical results on the NF–FF transformations with spiral scannings for quasi-spherical antennas [12], the two-dimensional OSI expansion, for reconstructing the voltage on the plane from a nonredundant number of its samples collected along the spiral, can be rigorously obtained by choosing the spiral in such a way that its pitch be equal to the sample spacing needed for the interpolation along a radial line and developing a nonredundant sampling representation along the spiral. The bandwidth, the parameter relevant to a radial line, and the related phase function are [7, 12]:

$$W_\eta = \beta a\,; \qquad \eta = \vartheta\,, \tag{1}$$

$$\psi = \beta\sqrt{r^2 - a^2} - \beta a \cos^{-1}\left(a/r\right), \tag{2}$$

β being the free-space wavenumber.

The sample spacing for the radial line interpolation and, as a consequence, the pitch of the spiral is then $\Delta\vartheta = 2\pi/(2N''+1)$, where $N'' = \mathrm{Int}(\chi N') + 1$, $\mathrm{Int}(x)$ denotes the integer part of x, $N' = \mathrm{Int}(\chi'\beta a) + 1$, and $\chi > 1$ is an oversampling factor, which controls the truncation error [7]. Accordingly, the equations of the spiral are:

$$\begin{cases} x = d\tan\theta\cos\phi = \rho\cos\phi \\ y = d\tan\theta\sin\phi = \rho\sin\phi \\ z = d \end{cases}, \tag{3}$$

where ϕ is the angular parameter describing the spiral. Moreover, the condition on the spiral pitch implies that $\theta = k\phi$, with $k = 1/(2N''+1)$ [12]. It is noteworthy that θ, unlike the zenithal angle ϑ, can take also negative values and that, when the spiral crosses the pole, the azimuthal angle φ has a discontinuity jump of π, while the spiral angle ϕ is continuous. Note that such a spiral can be viewed as obtained by radially projecting on the plane a proper spiral wrapping the sphere modelling the AUT.

As regards the nonredundant sampling representation along the spiral, it has been rigorously shown, in [11] for the planar spiral and in [12] for a spiral wrapping a quite arbitrary rotational surface, that the expressions of the phase function γ and of the parameter ξ are:

$$\gamma = \psi\,; \qquad \xi = \frac{\beta a}{W_\xi}\int_0^\phi \sqrt{k^2 + \sin^2 k\phi'}\,\mathrm{d}\phi'\,. \tag{4}$$

Accordingly, the parameter ξ is β/W_ξ times the curvilinear abscissa of the projecting point lying on the spiral that wraps the modelling sphere. The bandwidth W_ξ can be determined in such a way that the angle-like parameter ξ covers a 2π range when the whole projecting spiral on the sphere is described. As a consequence,

$$W_\xi = \frac{\beta a}{\pi}\int_0^{(2N''+1)\pi} \sqrt{k^2 + \sin^2 k\phi'}\,\mathrm{d}\phi'\,. \tag{5}$$

In light of the above results, the reduced voltage at the point P on the radial line at φ can be reconstructed by the following OSI expansion [11, 12]:

$$\tilde{V}(\vartheta, \varphi) = \sum_{n=n_0-q+1}^{n_0+q} \tilde{V}(\vartheta_n)\,\Omega_N\left(\vartheta - \vartheta_n, \bar{\vartheta}\right) D_{N''}(\vartheta - \vartheta_n), \tag{6}$$

wherein $2q$ is the number of the retained intermediate samples $\tilde{V}(\vartheta_n)$, namely, the reduced voltage values at the intersection points between the spiral and the radial line through P, $n_0 = \mathrm{Int}\left[(\vartheta - \vartheta_0)/\Delta\vartheta\right]$, $N = N'' - N'$, $\bar{\vartheta} = q\Delta\vartheta$, and

$$\vartheta_n = \vartheta_n(\varphi) = k\varphi + n\Delta\vartheta = \vartheta_0 + n\Delta\vartheta\,. \tag{7}$$

Moreover,

$$D_{N''}(\vartheta) = \frac{\sin\left((2N''+1)\vartheta/2\right)}{(2N''+1)\sin(\vartheta/2)}, \tag{8}$$

$$\Omega_N\left(\vartheta, \bar{\vartheta}\right) = \frac{T_N\left[-1 + 2\left(\cos(\vartheta/2)/\cos(\bar{\vartheta}/2)\right)^2\right]}{T_N\left[-1 + 2/\cos^2(\bar{\vartheta}/2)\right]}, \tag{9}$$

are the Dirichlet and Tschebyscheff sampling functions [7], where $T_N(\vartheta)$ is the Tschebyscheff polynomial of degree N.

The following OSI expansion along the spiral [11, 12] allows one to recover the intermediate samples:

$$\tilde{V}\left(\xi(\vartheta_n)\right) = \sum_{m=m_0-p+1}^{m_0+p} \tilde{V}(\xi_m)\,\Omega_M\left(\xi - \xi_m, \bar{\xi}\right) D_{M''}(\xi - \xi_m), \tag{10}$$

where $m_0 = \mathrm{Int}\left[\xi(\vartheta_n)/\Delta\xi\right]$, $2p$ is the number of the retained samples, $M = M'' - M'$, $\bar{\xi} = p\Delta\xi$, and

$$\xi_m = m\Delta\xi = 2\pi m/(2M''+1)\,, \tag{11}$$

with $M'' = \mathrm{Int}[\chi M'] + 1$ and $M' = \mathrm{Int}[\chi' W_\xi] + 1$.

Since small variations of ξ correspond to large changes of φ in the neighbourhood of the pole ($\vartheta = 0$), it is necessary to properly increase the factor χ' to avoid a significant growth of the bandlimitation error, when interpolating the voltage in this zone [11, 12].

It is so possible to accurately recover the voltages V_φ and V_ρ, acquired by the probe and rotated probe, at

the points required by the classical plane-rectangular NF–FF transformation [2]. Unfortunately, the probe corrected formulas in [2] (whose expressions in the here considered reference system can be found in [11]) are valid only if the probe maintains its orientation with respect to the AUT and this requires its co-rotation with it. To avoid such a co-rotation, a probe exhibiting only a first-order azimuthal dependence in its radiated far field can be used. In fact, in such a case, the voltages V_V and V_H (acquired by the probe and rotated probe with co-rotation) can be determined from V_φ and V_ρ via the relations:

$$V_V = V_\varphi \cos\varphi - V_\rho \sin\varphi \,;\; V_H = V_\varphi \sin\varphi + V_\rho \cos\varphi \,. \quad (12)$$

III. EXPERIMENTAL ASSESSMENT

In this section, some experimental results assessing the effectiveness of the described NF–FF transformation are shown. The tests have been performed in the anechoic chamber of the Antenna Characterization Lab of the University of Salerno, which is equipped with a plane-polar NF facility, besides the cylindrical and spherical ones. The amplitude and phase measurements are performed by using a vector network analyzer. The planar scanning is accomplished by mounting the AUT on a roll positioner and anchoring the probe (an open-ended WR90 rectangular waveguide) to a vertical scanner. The antenna employed in the experimental tests is a H-plane monopulse antenna, working in the sum mode at 10 GHz, located in the plane z = 0, and built by using a hybrid Tee and two pyramidal horns, whose apertures (8.9×6.8 cm sized) are at a distance of 26 cm between their centers. It has been modelled by a ball of radius a = 18.0 cm. The NF data are acquired along a spiral covering a circular zone of radius 110 cm on a plane at distance d = 50.5 cm from the AUT. The amplitudes of the recovered voltages V_φ and V_ρ relevant to the radial lines at φ = 0° and φ = 30° are compared in Figs. 2 and 3 with those directly measured. For completeness, the comparison between the recovered phase of V_φ on the radial line at φ = 0° and the directly measured one is also shown in Fig. 4. As can be seen, the reconstructions are very good, save for the zones characterized by very low voltage levels. These reconstructions have been obtained by choosing χ = 1.20 and $p = q$ = 7 to ensure a truncation error smaller than the measurement one [11]. Moreover, to make the aliasing error negligible, χ' has been chosen equal to 1.35, save for the zone of the spiral determined by the 24 samples centred on the pole, wherein it has been increased in such a way that the sample spacing is reduced by a factor 9.

At last, the FF patterns in the principal planes E and H, reconstructed from the NF data acquired along the spiral, are compared in Figs. 5 and 6 with those recovered via the classical cylindrical NF–FF transformation. As can be seen, a very good agreement results.

Note that the number of used spiral samples is 1 767 (1 575 regular + 192 extra samples) much smaller than those 21 609 and 33 581 needed by the classical plane-rectangular [2] and the Rahmat-Samii's plane-polar [5] NF–FF transformations, respectively.

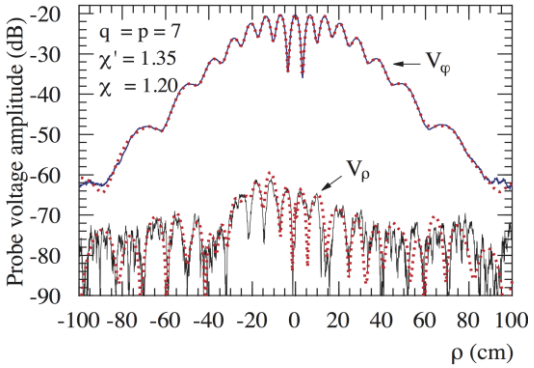

Fig. 2. Amplitudes of V_φ and V_ρ on the radial line at φ = 0°. Solid line: measured. Dashes: reconstructed from the NF data acquired along a spiral.

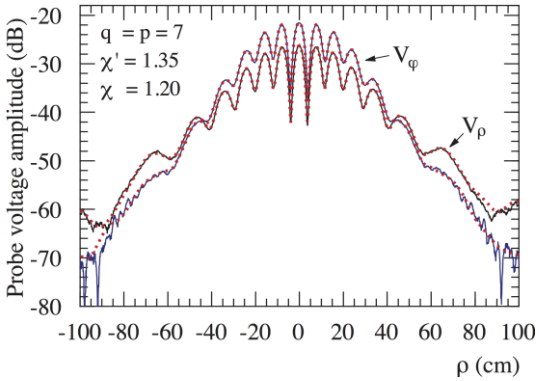

Fig. 3. Amplitudes of V_φ and V_ρ on the radial line at φ = 30°. Solid line: measured. Dashes: reconstructed from the NF data acquired along a spiral.

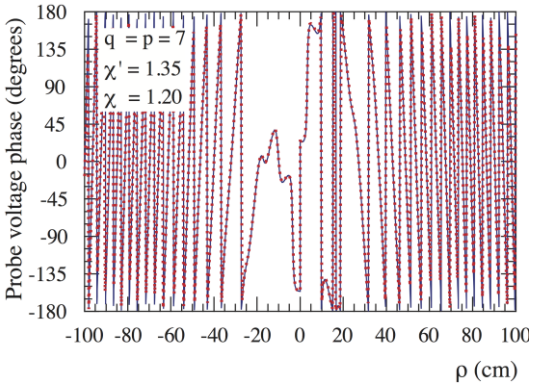

Fig. 4. Phase of V_φ on the radial line at φ = 0°. Solid line: measured. Dashes: reconstructed from the NF data acquired along a spiral.

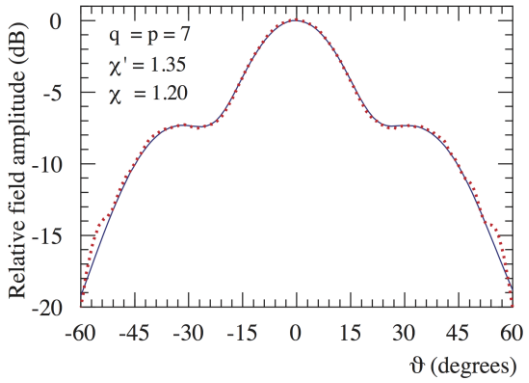

Fig. 5. E-plane pattern. Solid line: reconstructed from cylindrical NF data. Dashes: reconstructed from the NF data acquired along a spiral.

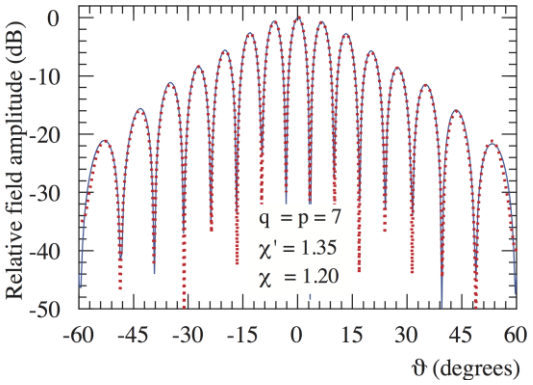

Fig. 6. H-plane pattern. Solid line: reconstructed from cylindrical NF data. Dashes: reconstructed from the NF data acquired along a spiral.

IV. CONCLUSION

An experimental validation of the described NF–FF transformation with planar spiral scan has been provided. The very good agreement found in the NF reconstructions, as well as that resulting from the comparison between the recovered FF patterns and those obtained by employing the cylindrical scanning, have fully confirmed its effectiveness also from the experimental viewpoint.

REFERENCES

[1] M. H. Francis, Ed., *IEEE Recommended Practice for Near-Field Antenna Measurements*, IEEE Standard 1720-2012.

[2] E. B. Joy, W. M. Leach, G. P. Rodrigue, and D. T. Paris, "Applications of probe-compensated near-field measurements," *IEEE Trans. Antennas Prop.*, vol. AP-26, pp. 379-389, May 1978.

[3] F. Ferrara, C. Gennarelli, R. Guerriero, G. Riccio, and C. Savarese, "An efficient near-field to far-field transformation using the planar wide-mesh scanning," *Jour. Electr. Waves Appl.*, vol. 21, pp. 341-357, 2007.

[4] F. D'Agostino, I. De Colibus, F. Ferrara, C. Gennarelli, R. Guerriero, and M. Migliozzi, "Far-field pattern reconstruction from near-field data collected via a nonconventional plane-rectangular scanning: Experimental testing," *Int. Jour. Antennas Prop*., vol. 2014, ID 763687, 9 pages, 2014.

[5] M. S. Gatti and Y. Rahmat-Samii, "FFT applications to plane-polar near-field antenna measurements," *IEEE Trans. Antennas Prop.*, vol. 36, pp. 781-791, June 1988.

[6] O. M. Bucci, C. Gennarelli, G. Riccio, and C. Savarese, "Near-field–far-field transformation from nonredundant plane-polar data: effective modellings of the source," *IEE Proc. Microw. Antennas Prop.*, vol. 145, pp. 33-38, Feb. 1998.

[7] O. M. Bucci, C. Gennarelli, and C. Savarese, "Representation of electromagnetic fields over arbitrary surfaces by a finite and non redundant number of samples," *IEEE Trans. Antennas Prop*., vol. 46, pp. 351-359, Mar. 1998.

[8] O. M. Bucci and C. Gennarelli, "Application of nonredundant sampling representations of electromagnetic fields to NF-FF transformation techniques," *Int. Jour. Antennas Prop*., vol. 2012, ID 319856, 14 pages, 2012.

[9] R. G. Yaccarino, L. I. Williams, and Y. Rahmat-Samii, "Linear spiral sampling for the bipolar planar antenna measurement technique," *IEEE Trans. Antennas Prop.*, vol. 44, pp. 1049-1051, 1996.

[10] S. Costanzo and G. Di Massa, "Near-field to far-field transformation with planar spiral scanning," *Prog. in Electr. Res.*, vol. 73, pp. 49-59, 2007.

[11] O. M. Bucci, F. D'Agostino, C. Gennarelli, G. Riccio, and C. Savarese, "Probe compensated far-field reconstruction by near-field planar spiral scanning," *IEE Proc. Microw. Antennas Prop.*, vol. 149, pp. 119-123, Apr. 2002.

[12] F. D'Agostino, C. Gennarelli, G. Riccio, and C. Savarese, "Theoretical foundations of near-field–far-field transformations with spiral scannings," *Prog. in Electr. Res.*, vol. 61, pp. 193-214, 2006.

[13] F. D'Agostino, F. Ferrara, C. Gennarelli, R. Guerriero, M. Migliozzi, "An effective NF-FF transformation technique with planar spiral scanning tailored for quasi-planar antennas," *IEEE Trans. Antennas Prop*., vol. 56, pp. 2981-2987, 2008.

[14] F. D'Agostino, F. Ferrara, C. Gennarelli, R. Guerriero, and M. Migliozzi, "The unified theory of near-field–far-field transformations with spiral scannings for nonspherical antennas," *Prog. in Electr. Res. B*, vol. 14, pp. 449-477, 2009.

[15] R. Cicchetti, F. D'Agostino, F. Ferrara, C. Gennarelli, R. Guerriero, and M. Migliozzi, "Near-field to far-field transformation techniques with spiral scannings: A comprehensive review," *Int. Jour. Antennas Prop*., vol. 2014, ID 143084, 2014.